Electronic Supplementary Material (ESI) for RSC Advances.

Electronic Supplementary Information

Redox Transformation Reaction for Hierarchical Hollow Au-MnOOH Flowers for High SERS Activity

Mukul Pradhan, Arun Kumar Sinha, Tarasankar Pal*

Department of Chemistry, Indian Institute of Technology, Kharagpur-721302, India

E-mail: tpal@chem.iitkgp.ernet.in

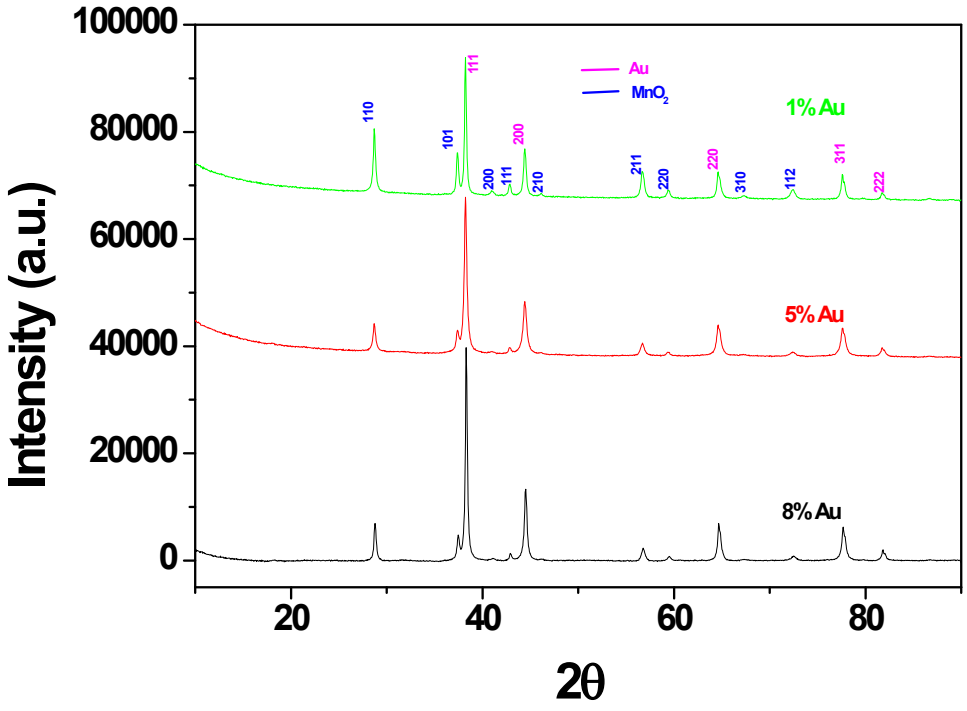

Figure S1. All the diffraction peaks of the product can be indexed to be Au doped *β*-MnO_2 obtained after calcination of Au-MnOOH at 350^0C. The XRD peaks can be well assigned to the planes 110, 101, 200, 111, 210, 211, 220, 310 and 112 for MnO_2 and 111, 200, 220, 311, and 222 for Au, respectively.

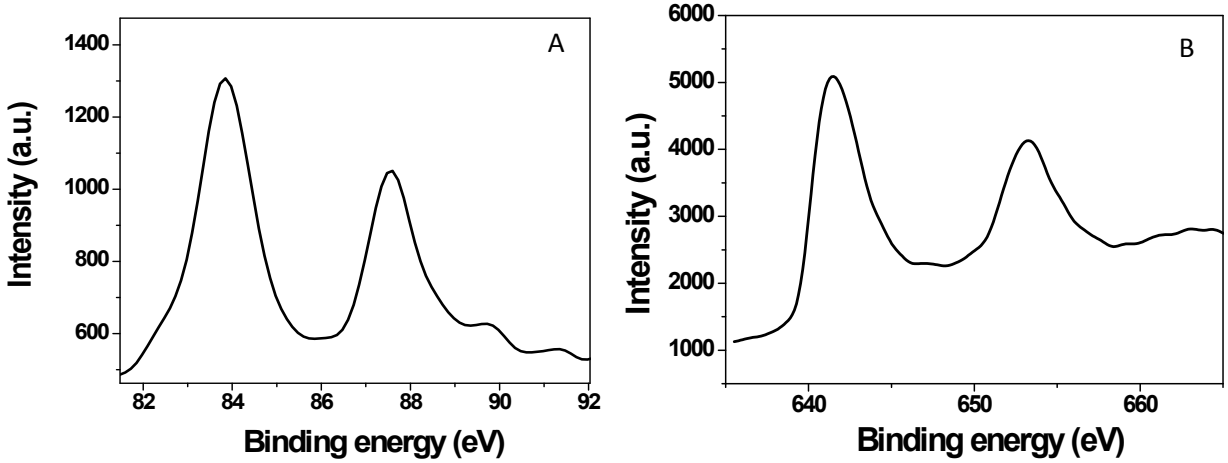

Figure S2. XPS pattern of the synthesized composite Au-MnOOH nanomaterials having 5 atomic percent Au: (A) for Au 4f and (B) for Mn 2p.

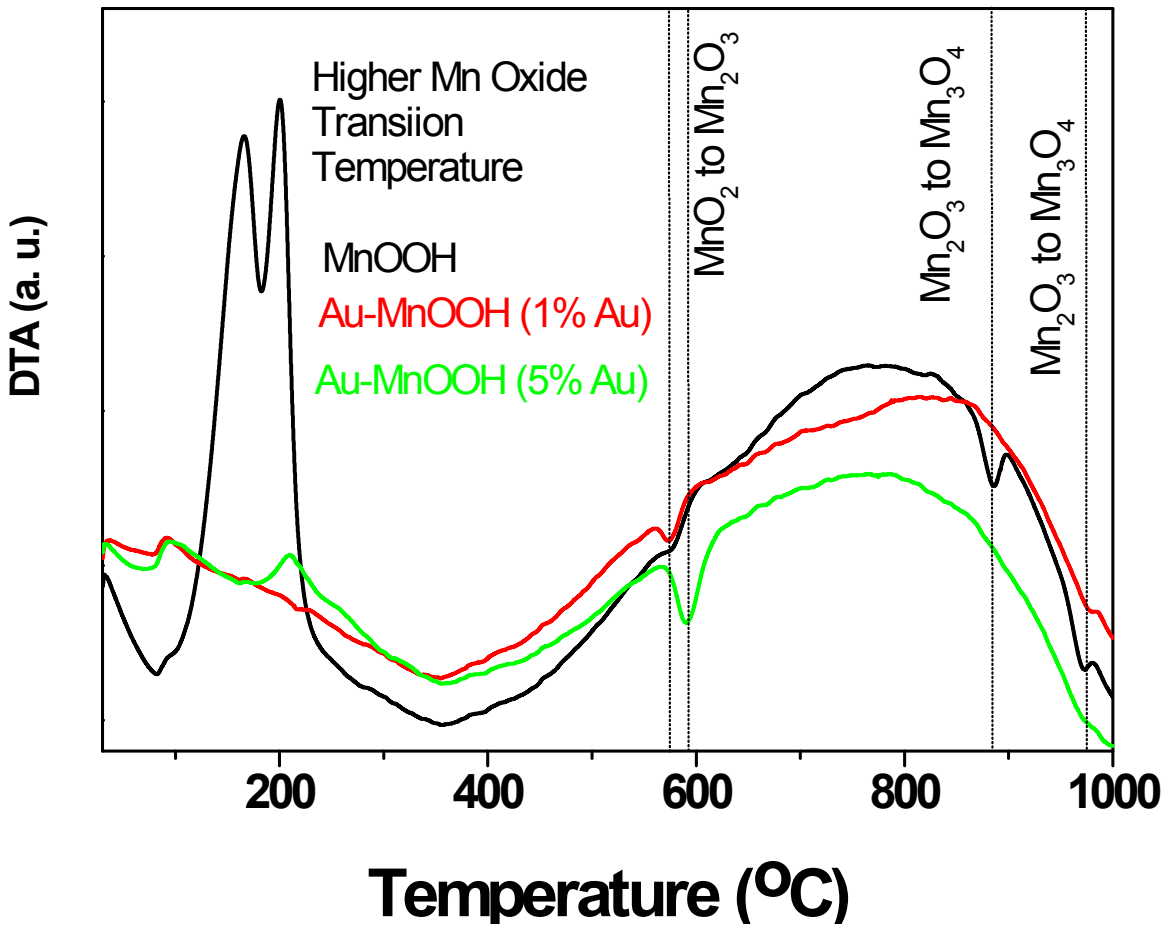

Figure S3. DTA curves in same window shows the gradual shift of manganese oxide transition temperature towards higher value for the Au-MnOOH composite in comparison to the pure MnOOH.

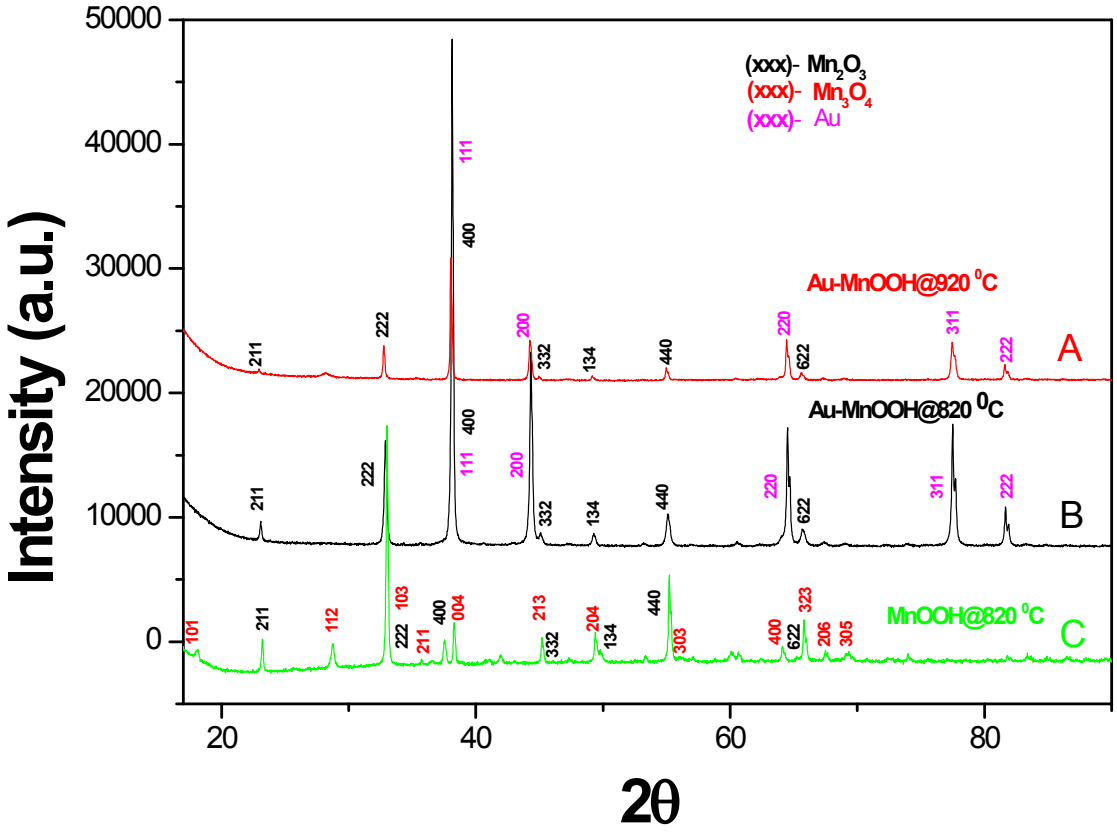

Figure S4. XRD pattern of annealed Au-MnOOH composite nanowires bearing 5% Au at 820^0 (B) and 920 ^{0}C (A). For the composition having Au (5%) remain stable as Mn_2O_3 even after annealing at 920 ^{0}C whereas pure MnOOH converts to Mn_3O_4 even at 820^0c (C).

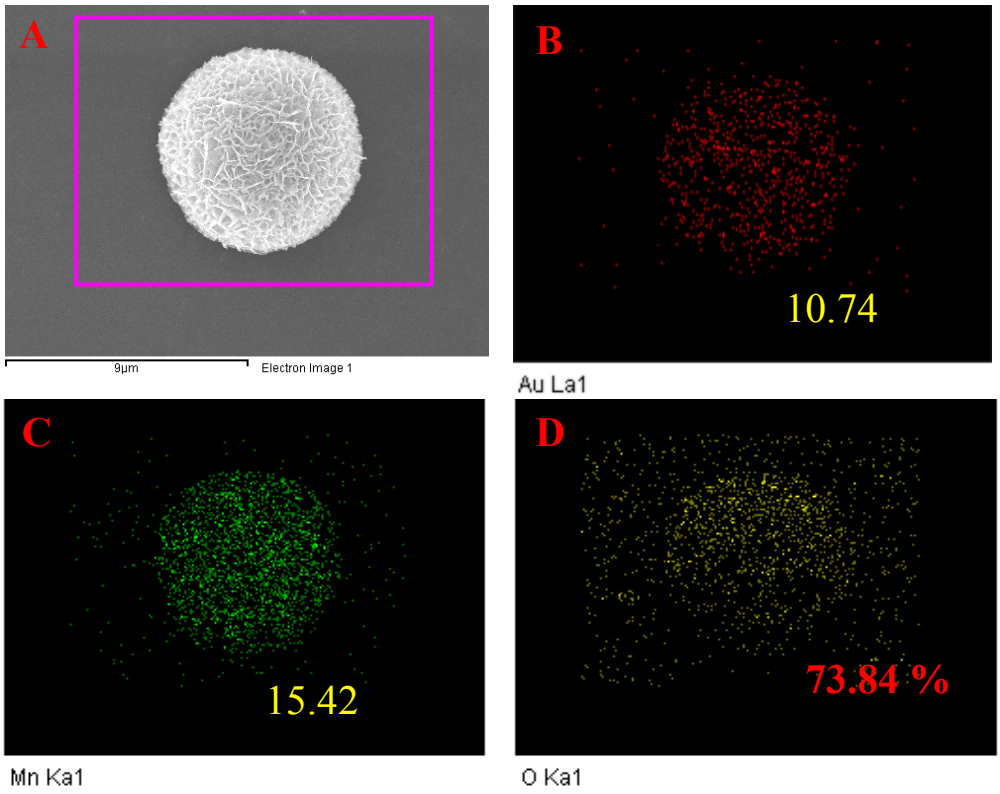

Figure S5. Elemental mapping (B-D) for each element from the marigold like Au-MnOOH flowery morphology (A) after 2 min.

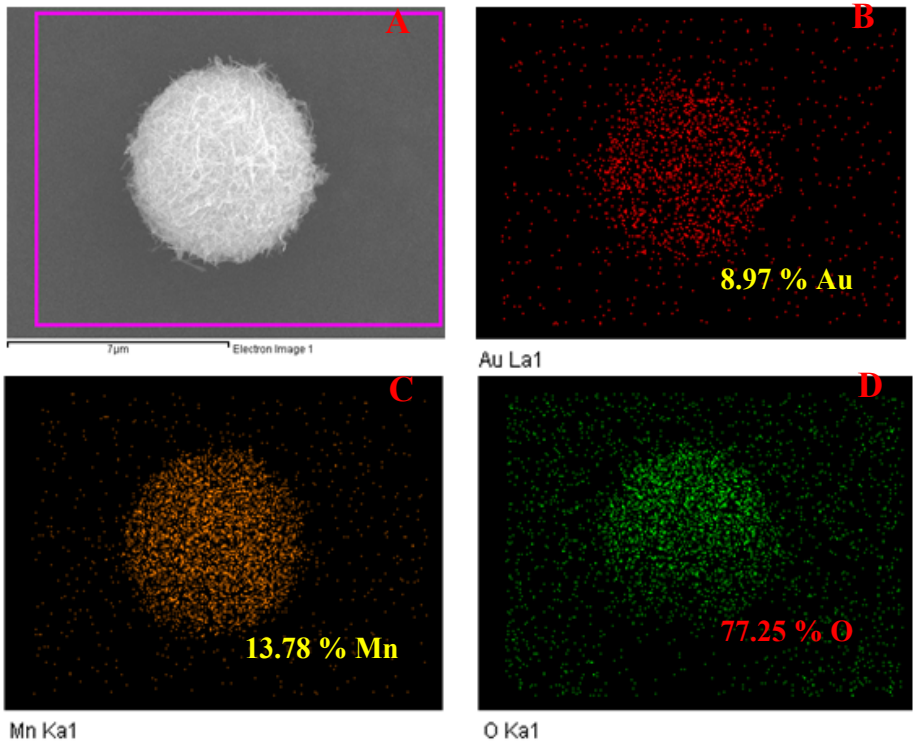

Figure S6. Elemental mapping (B-D) for each element from the marigold like Au-MnOOH flowery morphology (A) after 30 min.

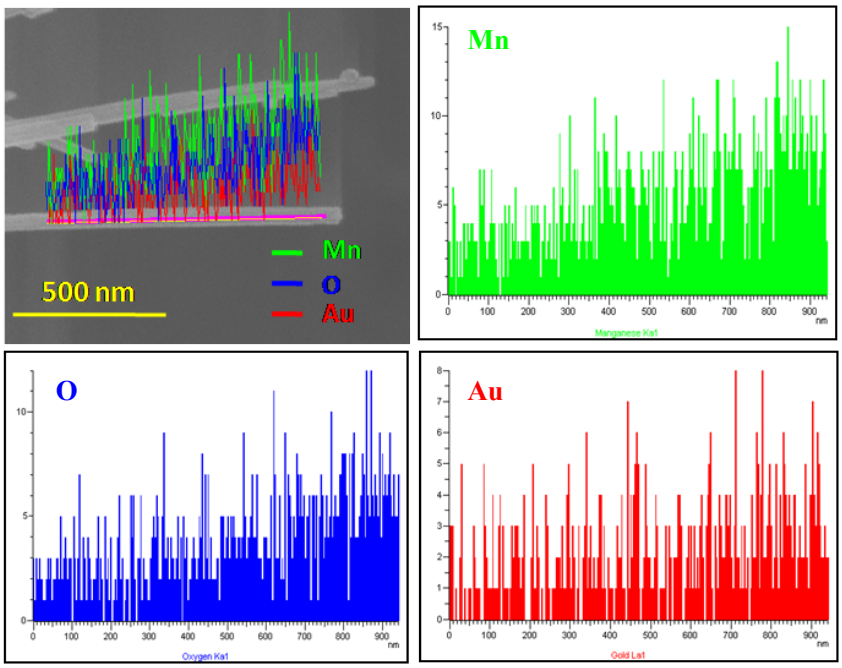

Figure S7. Line mapping from the EDX analysis for each element on the petal of Au-MnOOH flowery morphology having 8% Au.

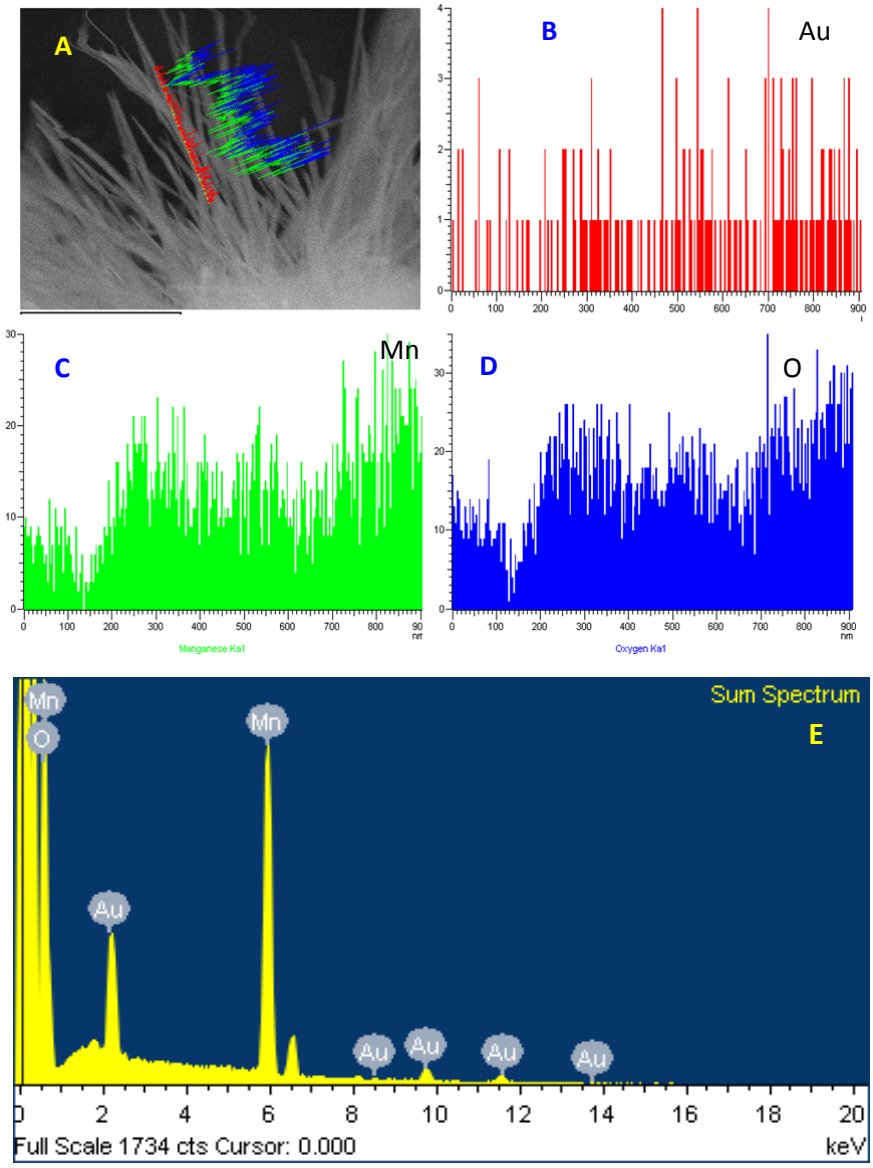

Figure S8: Line mapping (B-D) for each element on the petal of Au-MnOOH flowery morphology (A) and corresponding EDX spectra (D).

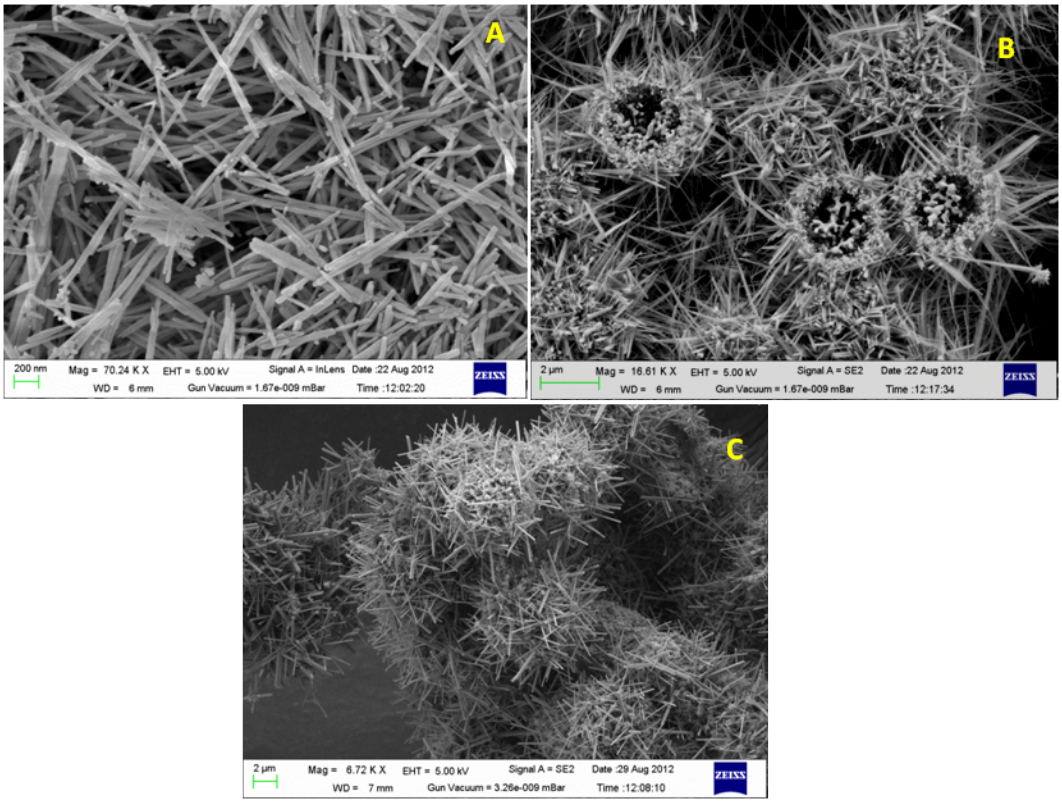

Figure S9. FESEM images of Au-MnOOH composite nanomaterials with different proportion of Au (A-C).

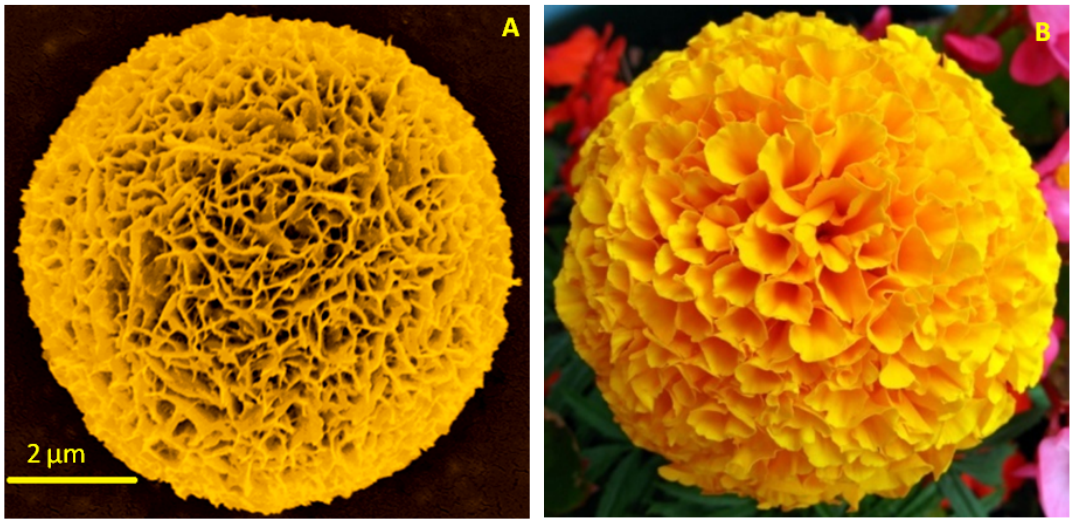

Figure S10. FESEM images of Au-MnOOH nanoflower (A) and digital photograph of natural marigold flower (B).

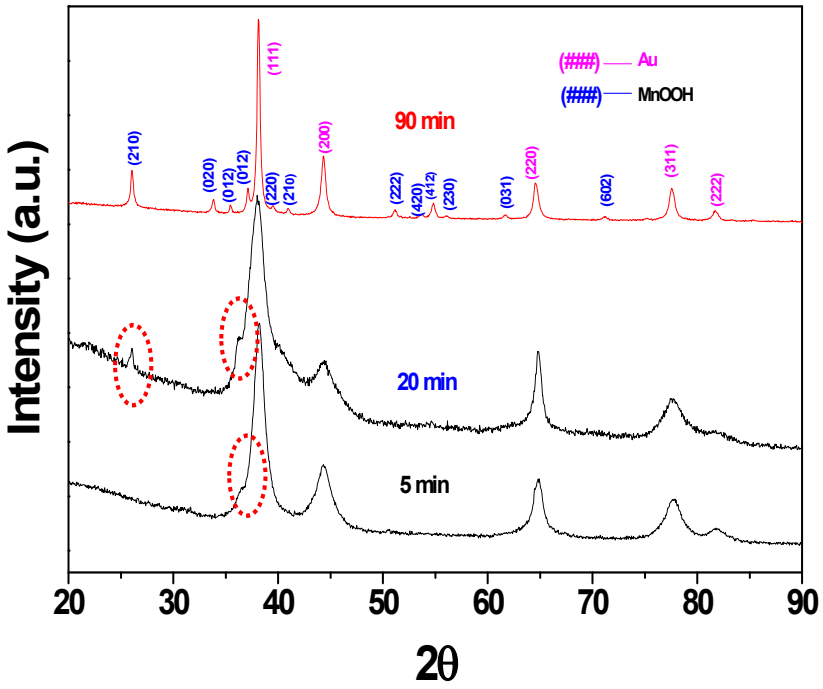

Figure S11: Time dependent XRD study during the formation of Au-MnOOH composite from $Mn(CH_3COO)_2$ and $HAuCl_4$. Encircled peaks indicate the gradual appearance of a crystalline phase of MnOOH.

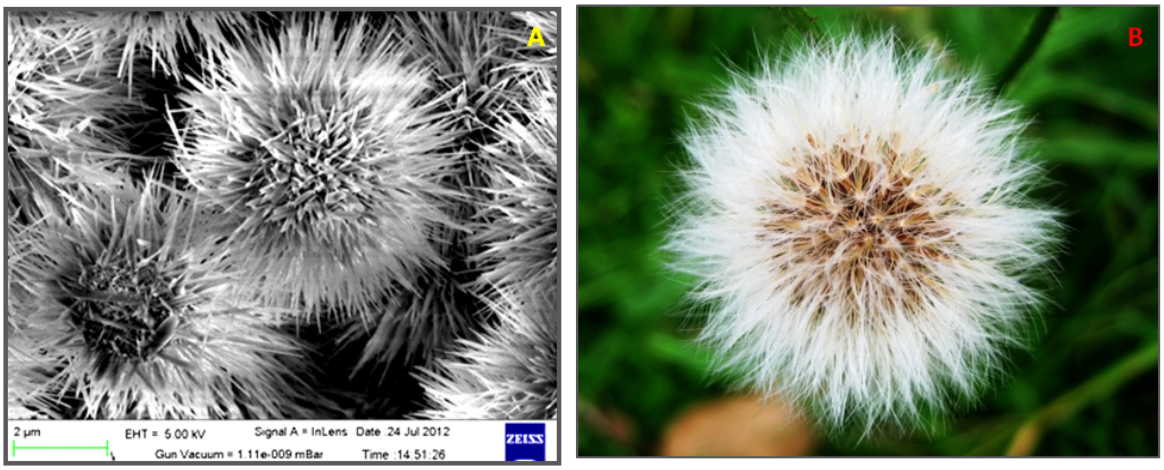

Figure S12. FESEM images of Au-MnOOH nanoflower (A) and digital photograph of natural dandelion flower (B).

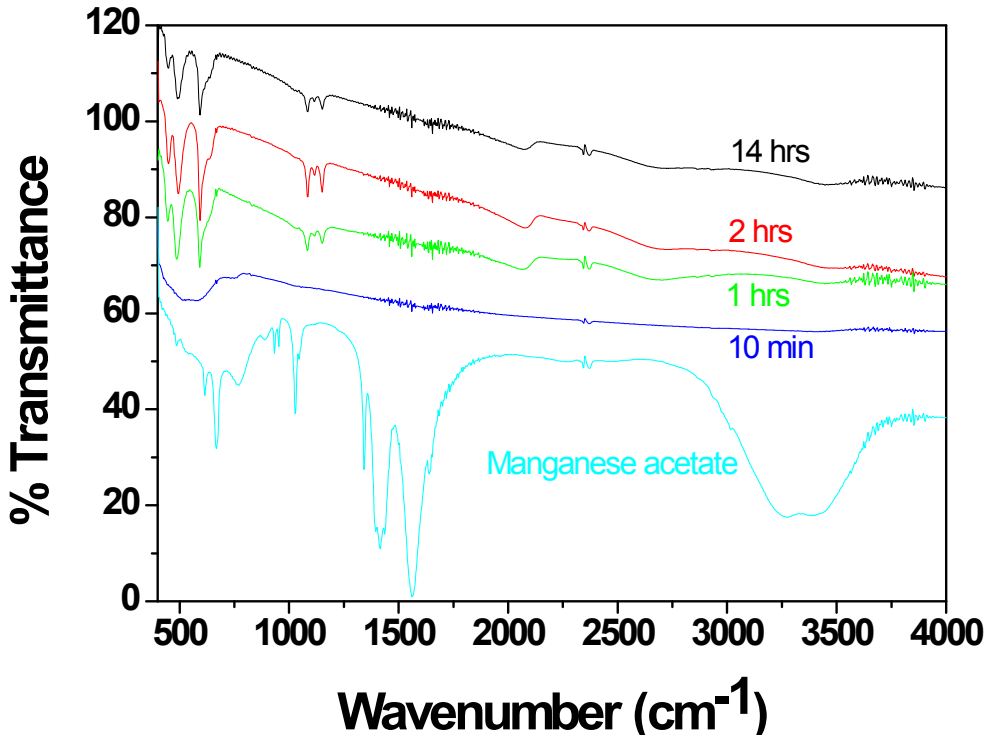

Figure S13. FTIR spectra of manganese acetate and time dependent growth of Ag-MnOOH.

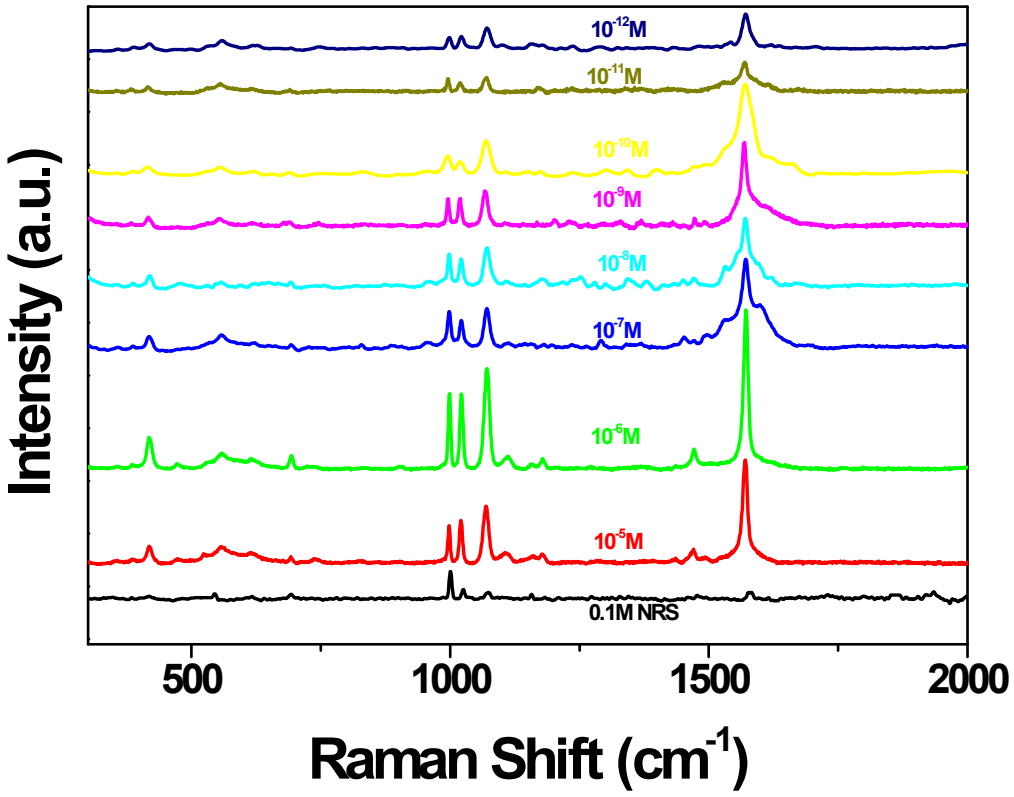

Figure S14. NRS spectrum of TP from 0.1 M in aqueous solution and SERS spectra of TP adsorbed on Au-MnOOH composite nanoflower at different concentrations of the adsorbate for λex = 632.8 nm.

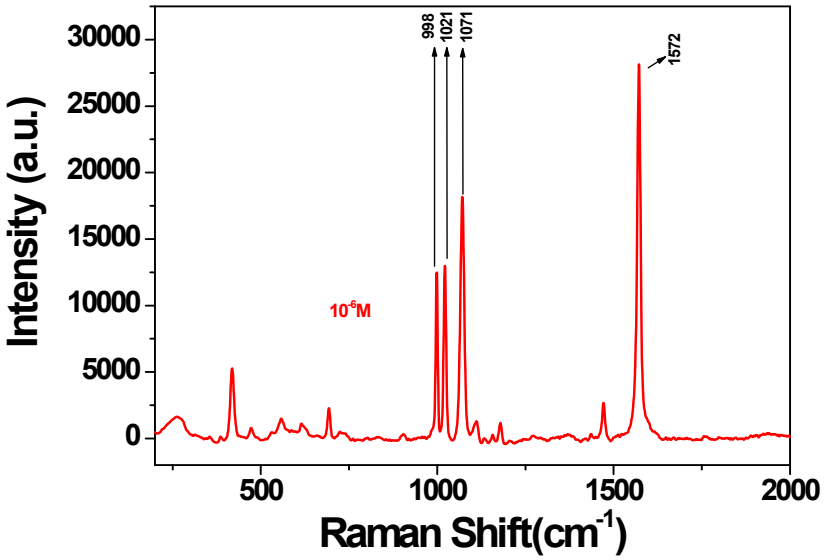

Figure S15. SERS spectra of thiophenol, TP (10^{-6} M) adsorbed on Au-MnOOH composite nanoflower for λ_{ex} = 632.8 nm.

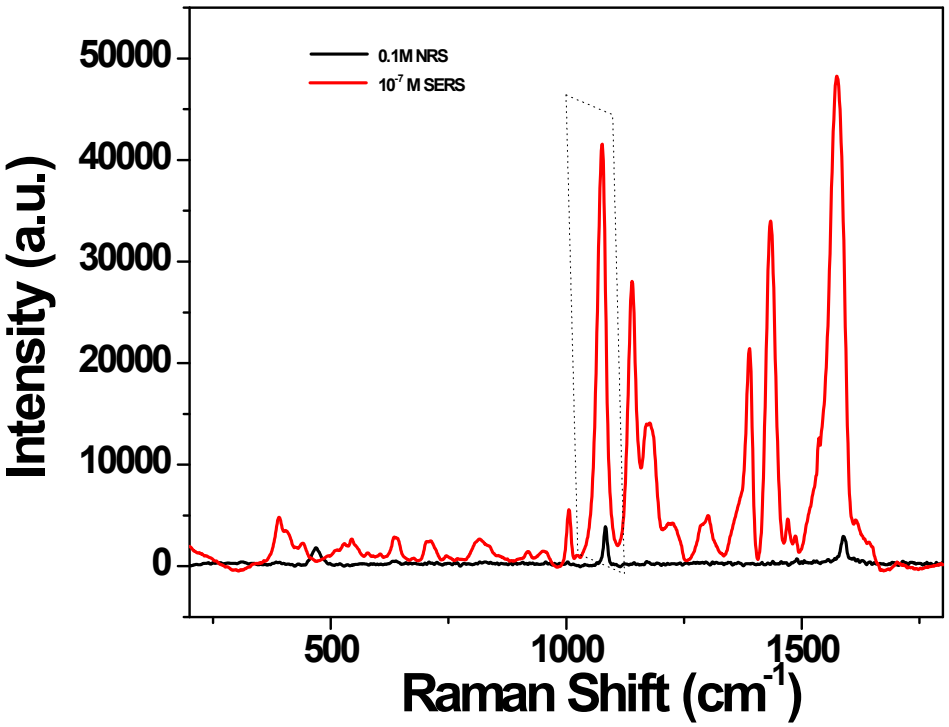

FigureS16. NRS spectra of ATP (0.1 M) and SERS spectra of 4-ATP (10^{-7}M) adsorbed on Au-MnOOH composite nanoflower.

AEF calculation taking 1083 cm^{-1} band from the above figure:

$AEF = \sigma_{SERS}[C_{NRS}] / \sigma_{NRS}[C_{SERS}]$

$=42024*0.1/3832*10^{-7}$

$=1.1*10^{7}$

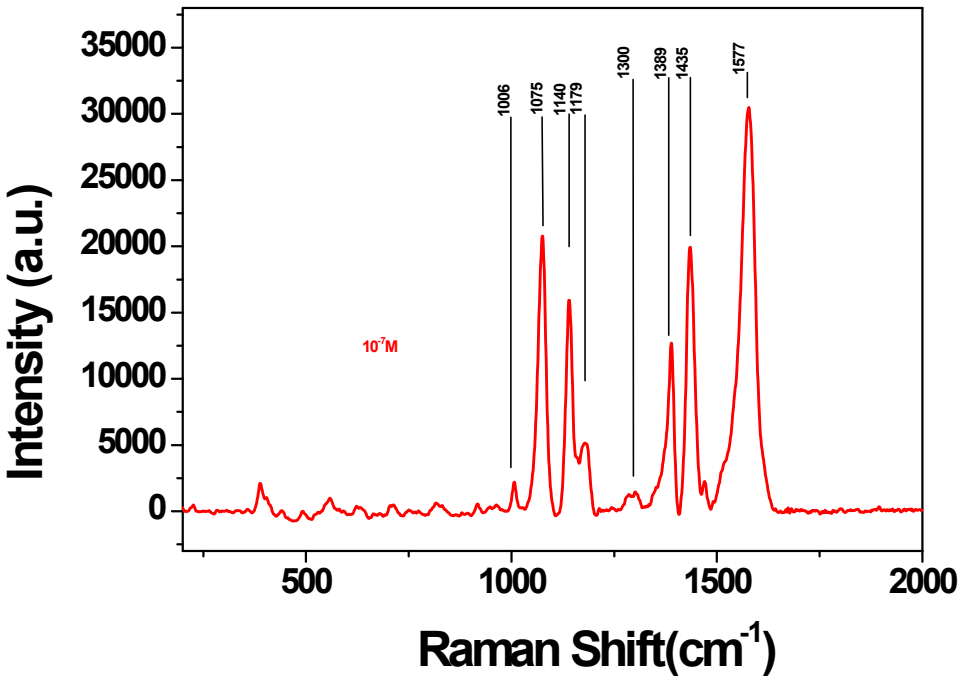

Figure S17. SERS spectra of 4-ATP adsorbed on Au-MnOOH composite nanoflower at 10^{-7} M adsorbate to characterize the band positions for λ_{ex} = 632.8 nm.

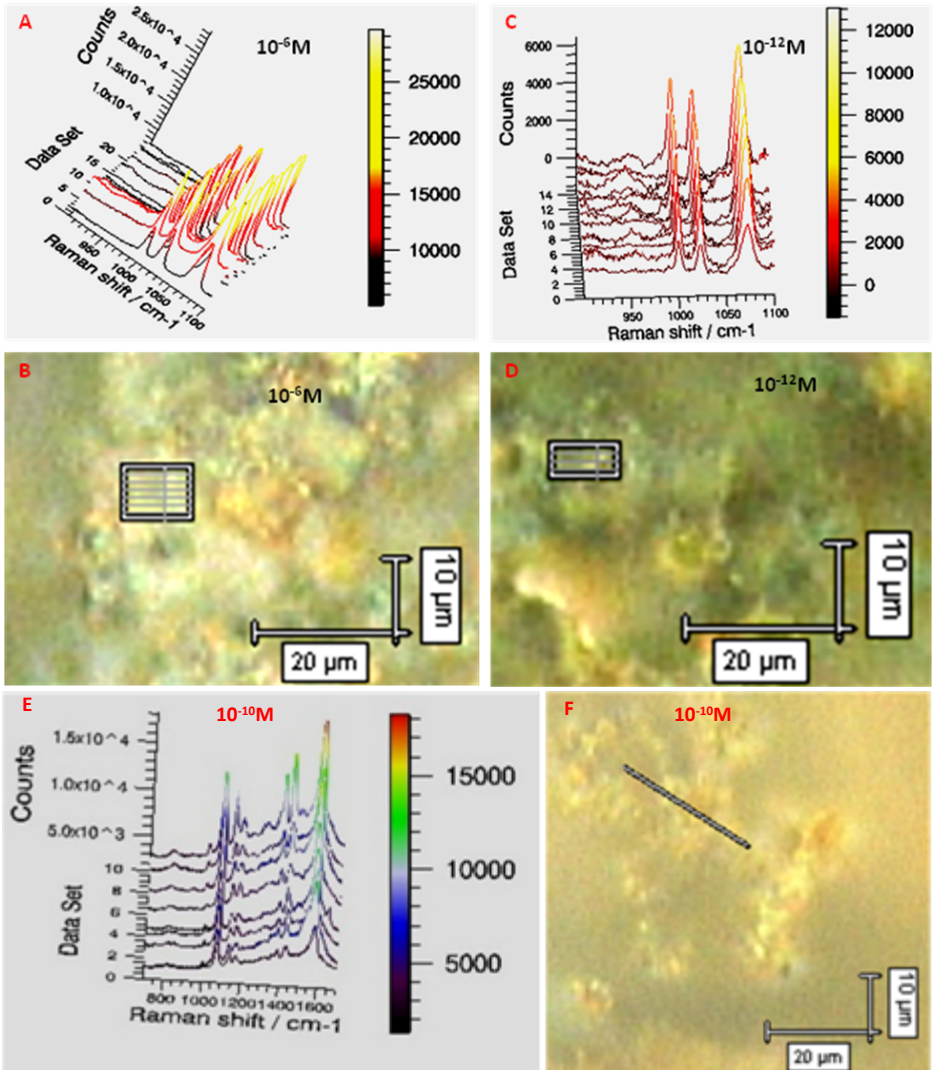

Figure S18. SERS spectra of selected bands from area mapping on Au-MnOOH nanoflower taking (A-D) TP and (E, F) 4-ATP as a probe molecule.

Table S1. Assignment of Vibrational Modes for Thiophenol Raman Peaks and Apparent Enhancement Factors (AEF) of Some Selected Raman Bands of Thiophenol Molecule Adsorbed on Au-MnOOH substrate

NRS, 0.1M (cm^{-1})	Symmetry	Assignment	SERS [10^{-5}M] (cm^{-1})	AEF X 10^5	SERS [10^{-6}M] (cm^{-1})	AEF X 10^6	SERS [10^{-7}M] (cm^{-1})	AEF X 10^7	SERS [10^{-11}M] (cm^{-1})	AEF X 10^{11}	SERS [10^{-12}M] (cm^{-1})	AEF X 10^{12}
418(w)	(a_1, a_2)	βCCC+ νCS	419	1.44	418	1.37	418	0.5	418	0.2	418	0.17
616 (ms)	b_1	βCCC +νCS	-----	-----	-----	-----	-----	-----	-----	-----	-----	-----
698	a_1	βCCC +νCS	-----	-----	-----	-----	-----	-----	-----	-----	-----	-----
1000(vvw)	a_1	βCCC	998	0.28	999	0.27	998	0.13	997	0.04	998	0.04
1025	a_1	βCH	1020	0.76	1022	0.81	1021	0.25	1020	0.12	1021	0.1
1072	b_1	βCH	1070	1.79	1071	1.64	1071	0.75	1070	0.27	1071	0.21
1157	b_1	βCH	-----	-----	-----	-----	-----	-----	-----	-----	-----	-----
1578	a_1&b_1	νCC	1571	2.37	1572	2.53	1571	1.71	1570	0.57	1572	0.37